

A model for fingerprint formation

M. KÜCKEN¹ and A. C. NEWELL^{1,2}

¹ *Program in Applied Mathematics, University of Arizona - 85721 Tucson, AZ, USA*

² *Department of Mathematics, University of Arizona - 85721 Tucson, AZ, USA*

received 14 April 2004; accepted in final form 27 July 2004

PACS. 87.18.La – Morphogenesis.

PACS. 87.19.Rr – Mechanical properties of tissues and organs.

Abstract. – The uniqueness of fingerprints (epidermal ridges) has been recognized for over two thousand years. They have been studied scientifically for more than two hundred years. Yet, in spite of the accumulation of a wealth of empirical and experimental knowledge, no widely accepted explanation for the development of epidermal ridges on fingers, palms and soles has yet emerged. Informed by an extensive literature study we suggest that fingerprint patterns are created as the result of a buckling instability in the basal cell layer of the fetal epidermis. Analysis of the well-known von Karman equations informs us that the buckling direction is perpendicular to the direction of greatest stress in the basal layer. We propose that this stress is induced by resistance of furrows and creases to the differential growth of the basal layer and regression of the volar pads during the time of ridge formation. These theories have been tested by computer experiments. The results are in close harmony with observations. Specifically, they are consistent with the well-known observation that the pattern type depends on the geometry of the fingertip surface when fingerprint patterns are formed.

A glance at one's own fingertips reveals a pattern of patches of almost parallel ridges with an almost constant crest-to-crest wavelength λ . The pattern is dominated by central features, such as whorls, loops, arches and triradii (see fig. 1 and corresponding simulations in fig. 2). Closer inspection reveals dozens of other imperfections such as ridge endings, ridge bifurcations, island ridges and others. The type and relative geometry of these dislocations is used by forensics for identification purposes [1, 2].

The crucial period of fingerprint development in humans starts at the 10th week of pregnancy [3–10]. At that time the epidermis (the outer layer of the skin) consists of three layers (periderm on the outside, the intermediate layer and the basal layer at the interface to the dermis) located on top of the dermis (the inner layer of the skin), which consists of amorphous tissue of fibroblasts and fibers. It is then observed that the basal layer of the epidermis becomes undulated toward the epidermis, forming what are called primary ridges. Primary ridges on the fingertip first appear along the nail furrow, the flexion crease and at one or two focal spots in the middle of the finger pad. From there they continue to spread over the remaining volar skin. Primary-ridge development ceases at about the 17th week of pregnancy. At this point the geometry of the epidermal-ridge system is determined for life and becomes visible on the skin surface in subsequent weeks.

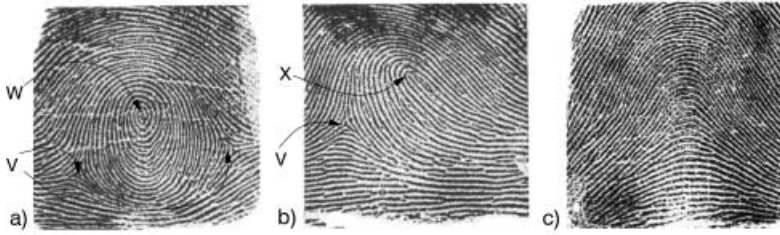


Fig. 1 – The most frequently occurring fingertip patterns: a) whorl, b) loop and c) arch. A whorl is characterized by a target/spiral (W) and two triradii (V, V), loops by a Roman arch structure (X) and one triradius (V).

It has long been appreciated that the developing pattern type is correlated to the so-called volar pads [11,12]. Volar pads are temporary eminences of the skin surface that form during the 7th week of pregnancy and start to digress at about the 10th week [13]. They are found at the fingertips, in the interdigital areas and sometimes in the hypothenar and thenar regions as well. From studies of embryos, monkeys and malformed hands, it has consistently been observed that highly rounded pads at the fingertips exhibit whorls; less well-developed pads show loops, where the direction of the loop opening is determined by the asymmetry of the pad; small indistinct pads give rise to arches [14,15]. This observed dependence of the pattern type on the fingertip geometry was used by Cummins to argue that the pattern is created by forces that are induced by differential growth [16]. Bonnevie argued that excessive growth of the basal layer results in compressive stress [4,17,18] leading to folding. Other theories to date have argued that epidermal ridges are induced by the pattern of incoming nerve axons [19,20] or by condensations in the dermis [21]; however, there are serious reservations about both [22]. In this letter, we demonstrate, for the first time, that a simple model based on the ideas of Cummins and Bonnevie yields results in close harmony with observations.

Much mathematical research on fingerprints has focused on their topological properties. It has been known for some time that loops and triradii and composites thereof such as whorls and dislocations are the canonical singularities of two-dimensional stripe patterns in translationally and rotationally invariant systems [23]. These singularities are characterized by a quantity called twist. The twist is defined as the anticlockwise angular rotation of a local wave director field whose direction is perpendicular to the ridge crest and whose amplitude is $2\pi/\lambda$. The twist around a loop singularity is π and the twist around a triradius is $-\pi$. By counting the twist along the margin of the hand in two ways, Penrose found a formula relating the number of loops L , the number of triradii T and the number of digits D in a simple formula ($L + D = T + 1$) [24,25].

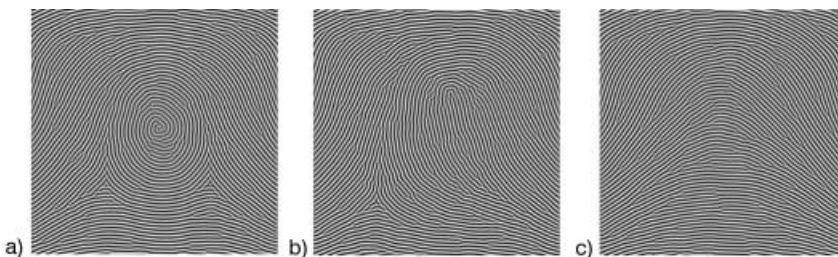


Fig. 2 – Simulations of the three common patterns: a) whorl, b) loop, c) arch.

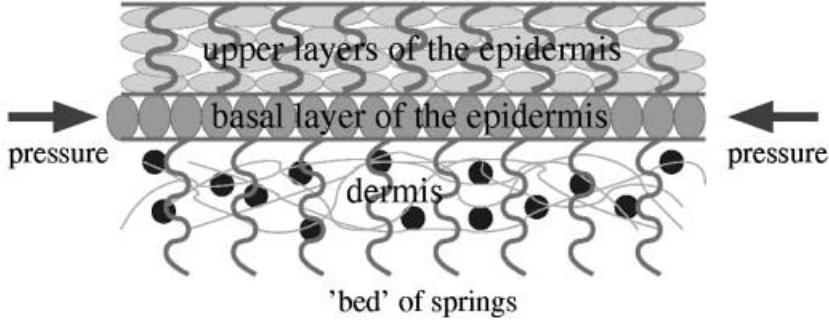


Fig. 3 – We consider the basal layer of the epidermis trapped between the intermediate layer and the dermis. Due to differential growth a compressive stress acts on the basal layer.

We consider the basal layer as an overdamped elastic sheet trapped between the neighboring tissues of the intermediate epidermis layer and the dermis that we model as beds of weakly non-linear springs (see fig. 3). Due to differential growth of the sheet and the constraints of the neighboring layers and boundaries a compressive stress is induced in the sheet. If the compressive stress is large enough, a buckling instability takes place. The balance between the bending resistance of the basal layer and the restoring forces of the elastic foundations establishes a finite wavelength. We analyze this buckling process by minimizing the total elastic energy of the system given by

$$\mathcal{E} = \int_A \left(\frac{D}{2} \nabla^2 w - \frac{1}{2Eh} \nabla^2 F + \frac{F_{yy}w}{R_x} + \frac{F_{xx}w}{R_y} - w[F, w] + V(w) \right) dx dy. \quad (1)$$

Here w denotes the normal deflection of the sheet and F the Airy stress function. E and D are Young's modulus and the bending modulus, respectively. Further, h denotes the shell thickness and R_x and R_y are the principal radii of curvature. The bracket is defined as follows:

$$[F, w] = F_{xx}w_{yy} + F_{yy}w_{xx} - 2F_{xy}w_{xy}. \quad (2)$$

Further,

$$V(w) = pw + \frac{\gamma w^2}{2} + \frac{\alpha}{3} w^3 + \frac{\beta}{4} w^4 \quad (3)$$

is a potential for the resistance of the surrounding tissues to normal displacements. In this expression, p denotes the normal pressure on the sheet, γ is the linear spring constant and α , β are non-linear spring constants.

The energy contains terms due to bending, in-plane deformations, normal pressure and normal spring resistance. Its functional derivatives give rise to a non-linear version of the well-known von Karman equations for curved surfaces [26]. Linear stability analysis of the equations reveals both that the buckling wavelength is too small to be caused by curvature effects and the intuitive result that the direction of the ridges will be roughly perpendicular to the direction of greatest stress. Non-linear analysis confirms that roll solutions (or ridges) are a stable solution of the equations. Hexagon (dot) solutions are stable under certain circumstances (low stress anisotropy, large quadratic interactions). Interestingly, such patterns are indeed observed on the palms of some marsupials.

To understand how the different fingerprint types form we now have to understand how stress is generated in the basal layer and how this process is related to the geometry. There are two central ideas. First, if the expansion of the basal layer is resisted in a certain direction,

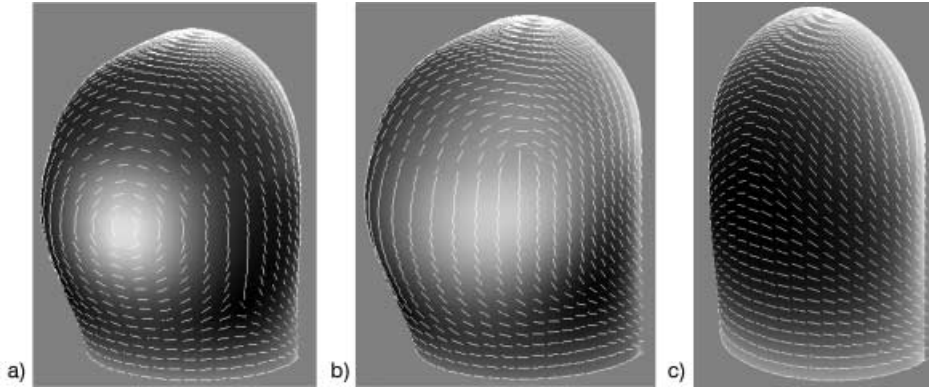


Fig. 4 – Boundary forces and normal load produce a stress field that, in many aspects, anticipates the future ridge pattern. Here, the direction of smallest stress is given (predicting the buckling direction). The color denotes the magnitude of largest compressive stress (white: large compressive stress, black: small compressive stress) and predicts the regions where ridge formation takes place first.

stress will form perpendicular to it and ridges will form parallel to the obstacle. The nail furrow and the major flexion creases of the finger and the palm are such obstacles. Indeed, ridges usually follow the outline of the nail and form along the mentioned creases. The second idea is connected with the regression of the volar pads at the time of fingerprint development and suggests why the geometry of the fingertips is so important for the pattern type. It is well known that normal displacements of curved surfaces toward the center of curvature produce compressive stress if tangential displacement is resisted [26]. Consider a well-rounded pad at the center of the fingertip. As the pad digresses (*i.e.* normal displacement takes place), compressive stress is generated in the radial direction from the center of the pad. Because the ridges align perpendicular to the greatest stress, a whorl naturally arises. For less pronounced pads, the greatest curvature in the fingertip center is perpendicular to the axis of the finger and gives rise to compressive stress in that direction. Accordingly, the ridges follow the axis of the finger in the fingertip center and give rise to a loop. The type of asymmetry in the loop is determined by the asymmetry of the volar pad and has been verified in computer simulations. If the pad is flat and no more regression takes place, then the stress distribution in the middle of the pad is solely influenced by the expansion resistance from the boundary and an arch forms. In order to conserve twist, the merging of the ridges arising in the pad center with the patches induced by the nail boundary and flexion crease leads to the corresponding number of triradii (two for a whorl, one for a loop). Not only does this reasoning establish the correct pattern for the given geometry but it also confirms that the fingertip pattern will first form at the nail furrow, the flexion crease and the middle of the pad where regression is greatest (see fig. 5).

The ideas presented above were tested by analysis and computer simulations. Because the complete buckling problem of the curved fingertip is too complex for efficient numerical analysis, we performed the simulations in two steps. In the first step, using finite elements, boundary and normal forces were imposed on a fingertip model, yielding the in-plane stress distribution. The boundary forces in all the simulations were the same (pointing inwards at the nail furrow and the flexion crease). However, different geometries (highly rounded for whorl, less rounded and asymmetric for loop, flat for arch) and different normal loads (large and symmetric for whorl, less strong and asymmetric for loop, small for arch) were used. The resulting stress field is locally not isotropic; therefore, when buckling occurs, the resulting ridges run perpendicular to the direction of local maximum stress. The results can be seen in fig. 4. The stress field

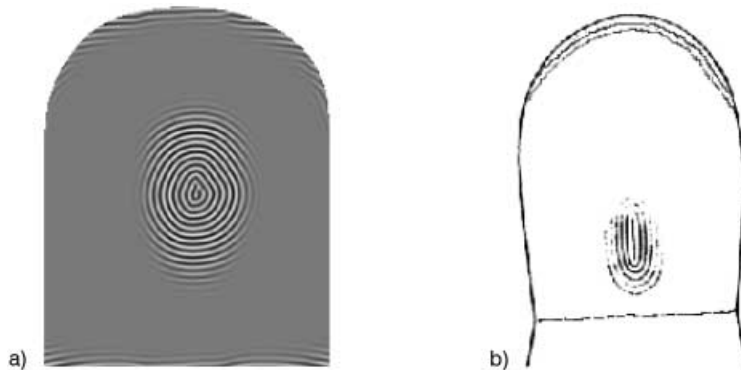


Fig. 5 – In a), our simulation, the pattern begins to emerge at the boundaries (nail furrow, crease) and at the center of the volar pad. This is consistent with b), the experimental observation of Bonnevie [4].

anticipates the direction of the ridge system and also predicts in what areas buckling will take place first. These are the areas of highest compressive stress shown in light colors in fig. 4. In the second step, we used the von Karman equations to calculate the buckling pattern. The stress field obtained in the first step was projected to the plane (with the necessary compromises) and used to parameterize the von Karman equations. Here we took advantage of the fact that the buckling wavelength is small compared to distances over which the prebuckling stress varies. The stress was raised over critical stress and the resulting pattern recorded.

The results we obtain are most encouraging. We capture the formation of whorls, loops and arches as well as the correct pattern textures (fig. 2). A multitude of dislocations arise in regions where ridge patches with different directions meet and are the results of the melding patches attempting to keep the pattern wavelength close to its preferred value. Furthermore, the number of dislocations depends on how much the compressive stress in the basal layer exceeds the stress necessary for the buckling instability. In our simulations this number approximately corresponds to the number observed on most fingers (about 100–150). This number increases with the stress parameter in a manner consistent with the observations of Hale [27].

In fig. 2, we show the results of three simulations arising from conditions whose aim is to replicate the three real patterns shown in fig. 1. In fig. 2a), we applied normal pressure at the center of a highly rounded finger pad in order to simulate the compressive stress that is formed during pad regression. In fig. 2b) the pad was asymmetric and not as rounded and the applied stress smaller. In fig. 2c), there was little central pressure and the ridge direction is mostly influenced by the resistance to expansion at the flexion crease and the nail furrow. In fig. 5a), we examine the onset of the epidermal-ridge pattern and compare it to Bonnevie's observations in fig. 5b). Note how the epidermal-ridge pattern, in reality and the simulation, first appears at the nail furrow, the flexion crease and the whorl center. More details are given in [22].

The main difference between observations and simulations is the appearance of amplitude grain boundaries (closely packed dislocations) in the latter as seen, for example, near the triradii in fig. 2a). This would suggest that real epidermal ridges are formed in a less rigid medium in which small plastic and viscoelastic influences allow the constraint of a preferred wave number to be loosened a little so that dislocations are more separated.

Apart from getting a better understanding of the embryological processes of epidermal-ridge formation, this work could be important for giving forensic fingerprint identification a more solid foundation. For example, our model allows us to study to what extent small random disturbances influence the ridge pattern. This way we can find quantitative measures of fingerprint individuality.

Somewhat related to our efforts are models that attempt to reproduce realistic-looking fingerprints without using embryological observations [28]. Similar as in our work a direction field for the ridges is established first on which the ridge pattern is then superimposed. The results of this approach look quite convincing, in part because they allow for a gradual change in the wavelength that smoothes the flow of the ridges. However, like all approaches purely based on the final appearance of the epidermal-ridge system they do not illuminate the actual physical processes during ridge formation *in utero*. Other references of interest in this field are [29–31].

* * *

We thank P. SHIPMAN for discussions. We appreciate support from NSF grant DMS 0202440.

REFERENCES

- [1] CUMMINS H. and MIDLO C., *Fingerprints, Palms and Soles* (Research Publishing Company) 1976.
- [2] GALTON F., *Finger Prints* (Macmillan and Co.) 1892.
- [3] BABLER W., *Dermatoglyphics: Science in Transition*, edited by PLATO C., GARRUTO R. and SCHAUMANN B., Vol. **9** (Wiley-Liss) 1991, p. 95.
- [4] BONNEVIE K., *Nyt Mag. Naturvidensk.*, **65** (1927) 19.
- [5] GOULD E. S., *A topographic study of the differentiation of the dermatoglyphics in the human embryo*, PhD Thesis (Tulane University) 1948.
- [6] HALE A. R., *Am. J. Anat.*, **91** (1951) 147.
- [7] HIRSCH W., *J. Ment. Defic. Res.*, **17** (1973) 58.
- [8] OKAJIMA M., *J. Med. Genet.*, **12** (1975) 243.
- [9] PENROSE L. S. and O'HARA P. T., *J. Med. Genet.*, **10** (1973) 201.
- [10] SCHAEUBLE J., *Z. Morphol. Anthropol.*, **31** (1932) 403.
- [11] WHIPPLE I., *Z. Morphol. Anthropol.*, **7** (1904) 261.
- [12] SCHLAGINHAUFEN O., *Morphol. Jahrb.*, **33** (1905) 577.
- [13] CUMMINS H., *Contrib. Embryol.*, **20** (1929) 105.
- [14] BONNEVIE K., *Z. Indukt. Abstamm. Ver.*, **50** (1929) 219.
- [15] MULVIHILL J. J. and SMITH D. W., *J. Pediatr.*, **75** (1969) 579.
- [16] CUMMINS H., *Am. J. Anat.*, **38** (1926) 89.
- [17] BONNEVIE K., *Roux Arch. Dev. Biol.*, **117** (1927) 384.
- [18] BONNEVIE K., *Roux Arch. Dev. Biol.*, **126** (1932) 348.
- [19] DELL D. A. and MUNGER B. L., *J. Comp. Neurol.*, **244** (1986) 511.
- [20] MOORE S. J. and MUNGER B. L., *Dev. Brain Res.*, **48** (1989) 119.
- [21] BENTIL D. E. and MURRAY J. D., *Physica D*, **63** (1993) 161.
- [22] KÜCKEN M., *On the formation of fingerprints*, PhD Thesis (University of Arizona) 2004.
- [23] PASSOT T. and NEWELL A. C., *Physica D*, **74** (1994) 301.
- [24] PENROSE L. S., *Birth Defects, Orig. Artic. Ser.*, **4** (1968) 1.
- [25] PENROSE R., *Ann. Hum. Genet.*, **42** (1979) 435.
- [26] GOULD P. L., *Analysis of Plates and Shells* (Prentice Hall) 1999.
- [27] HALE A. R., *Anat. Rec.*, **105** (1949) 763.
- [28] CAPPELLI R., *Handbook of Fingerprint Generation*, edited by MALTONI D., MAIO D., JAIN A. K. and PRABHAKAR S. (Springer) 2003, p. 203.
- [29] SHERLOCK B. and MONRO D., *Pattern Recognition*, **26** (1993) 1047.
- [30] VIZCAYA P. and GERHARDT L., *Pattern Recognition*, **29** (1996) 1221.
- [31] SHERSTINSKY A. and PICARD R. W., *Proceedings of the 12th ICPR* (IEE Computer Society Press, Los Alamitos, Cal.) 1994, p. 195.